NASA/TM—2001-211218

The Tensile Properties of Advanced Nickel-Base Disk Superalloys During Quenching Heat Treatments

Timothy P. Gabb and John Gayda
Glenn Research Center, Cleveland, Ohio

Pete T. Kantzos
Ohio Aerospace Institute, Brook Park, Ohio

Tiffany Biles
Purdue University, West Lafayette, Indiana

William Konkel
Wyman-Gordon Forgings, Houston, Texas

Prepared for the
2001 Fall Meeting
sponsored by The Minerals, Metals, and Materials Society
Indianapolis, Indiana, November 4–8, 2001

National Aeronautics and
Space Administration

Glenn Research Center

October 2001

Acknowledgments

The authors wish to acknowledge the many helpful discussions with David Mourer at General Electric Aircraft Engines. The tests were performed at Wyman-Gordon, Houston, R&D Lab, by Mike Powell, while the heat treatments were performed by Jimmy Arnold.

THE TENSILE PROPERTIES OF ADVANCED NICKEL-BASE DISK SUPERALLOYS DURING QUENCHING HEAT TREATMENTS

Timothy P. Gabb and John Gayda
National Aeronautics and Space Administration
Glenn Research Center
Cleveland, Ohio 44135

Pete T. Kantzos
Ohio Aerospace Institute
Brook Park, Ohio 44142

Tiffany Biles
Purdue University
West Lafayette, Indiana 47907

William Konkel
Wyman-Gordon Forgings
Houston, Texas 77095

Abstract

There is a need to increase the temperature capabilities of superalloy turbine disks. This would allow full utilization of higher temperature combustor and airfoil concepts under development. One approach to meet this goal is to modify the processing and chemistry of advanced alloys, while preserving the ability to use rapid cooling supersolvus heat treatments to achieve coarse grain, fine gamma prime microstructures. An important step in this effort is to understand the key high temperature tensile properties of advanced alloys as they exist during supersolvus heat treatments. This could help in projecting cracking tendencies of disks during quenches from supersolvus heat treatments. The objective of this study was to examine the tensile properties of two advanced disk superalloys during simulated quenching heat treatments. Specimens were cooled from the solution heat treatment temperatures at controlled rates, interrupted, and immediately tensile tested at various temperatures. The responses and failure modes were compared and related to the quench cracking tendencies of disk forgings.

INTRODUCTION

The advanced powder metallurgy disk alloy ME3 was designed in the NASA High Speed Research/Enabling Propulsion Materials program to have extended durability at 600-700°C in large disks. This was achieved by designing a disk alloy with moderately high refractory element levels optimized with supersolvus heat treatments to produce balanced monotonic, cyclic, and time-dependent mechanical properties. The resulting baseline alloy, processing, and supersolvus heat treatment has been shown to

produce extended durability properties. This alloy has robust processing characteristics (ref. 1), with good resistance to cracking during quenches at moderately rapid cooling rates after supersolvus heat treatments.

The advanced disk alloy Alloy 10 was designed through modifications of an earlier alloy, AF115, by Textron-Lycoming (now Honeywell) in several programs to allow maximum regional engine performance at temperatures up to 700°C in smaller disks. This was achieved by using higher levels of refractory elements optimized with modern powder and billet production practices and subsolvus heat treatments using rapid cooling rates to produce maximum tensile and creep strength (ref. 2). However, the application of supersolvus heat treatments with moderately rapid quench cooling rates to Alloy 10 has produced cracks during quenching of even small disks (ref. 3).

There is a long-term need for disks with higher rim temperature capabilities of 760°C or more. This would allow higher compressor exit (T3) temperatures and allow the full utilization of advanced combustor and airfoil concepts under development. It has been shown that faster quenching rates can improve tensile and creep resistance in many disk alloys (ref. 4-6). It is therefore important to understand the key differences in high temperature tensile properties of the two alloys during supersolvus heat treatments, which could possibly explain the differences in their quench cracking capabilities. An "on-cooling" tensile testing technique has been developed to help understand these properties (ref. 7). This test strives to capture the transient properties and microstructures of the disk material during quenching from the solution heat treatment.

The objective of this study was to compare the tensile properties of two disk superalloys, ME3 and Alloy 10, during simulated quenching heat treatments. Specimens were cooled from the solution heat treatment temperatures at controlled rates, interrupted, and immediately tensile tested at various cooling temperatures. The responses were compared and related to the quench cracking tendencies of small disk forgings of these two alloys.

MATERIALS AND PROCEDURE

Forging and heat treatment of disks were performed by Wyman-Gordon Forgings, Houston, Texas. Heat treatments of specimen blanks were performed at Wyman-Gordon Forgings and NASA Glenn Research Center. Specimen machining and testing were performed by Wyman-Gordon. Sections of ME3 extrusion were machined and forged into disks about 12-17 cm diameter and 4cm thick. Sections of Alloy 10 extrusions were machined and forged into larger disks about 30 cm diameter and 5 cm thick. The two alloys were forged to the same upset and effective strain. Specimen blanks were machined using electro-discharge machining from one forging of each alloy, and then solution heat treated..

Solution heat treatment complexity and soak time effects were studied in ME3. ME3 blanks were either given a short, simple "direct heatup" (DH) supersolvus heat treatment of 1171°C/1h/air cool or a more extended, two-step "pre-annealed" (PA) heat treatment sequence of 1115°C/1h subsolvus pre-anneal+ 1171°C/3h supersolvus solution heat treatment, then air cooled. Alloy 10 blanks were all given a similar subsolvus pre-anneal plus supersolvus solution heat treatment of 1135°C/1h+1200°C/2.5h/air cool.

Tensile specimens were then machined with a gage diameter of 0.63 cm and gage length of 1.9 cm.

The specimens were then heated and tensile tested in a servohydraulic test system employing direct resistance heating and a diametral extensometer. In the tensile tests, specimens were first heated back up to their supersolvus solution heat treatment temperature and stabilized there for 5-10 minutes. They were then cooled at a controlled cooling rate to the test temperature, stabilized for about 20 seconds, and finally tensile tested to failure. All ME3 and a majority of the Alloy 10 specimens were cooled at a target rate of about 278°C/min. to the test temperature. Four other Alloy 10 specimens were cooled at a slower rate of about 69°C/min. to briefly assess cooling rate effects.

The tensile tests were run in general accordance with ASTM E21, using two sequential test segments at slow, then faster strain rates. However, each test was initially controlled using a constant radial strain rate, rather than axial strain rate. Axial strain was estimated as 2*radial strain. An initial axial strain rate of 0.0008 s^{-1} was employed. For specimens which continued to 1% radial strain, tests were then continued to failure at a controlled axial displacement rate of 0.025 cm/s. The extensometer remained on the specimen, and indicated an average axial strain rate of about 0.03 s^{-1}.

Fracture surfaces of selected specimens and quench cracks from previously heat treated disk forging sections were evaluated by scanning electron microscopy. Cracking modes and grain sizes were also examined on fracture surfaces and metallographically sections prepared on a longitudinal plane parallel to the loading direction. Grain sizes were determined according to ASTM E112 linear intercept procedures using circular grid overlays.

RESULTS AND DISCUSSION

Tensile Stress-Strain Response

1. Comparison of Tensile Stress-Strain Curves

The stress-strain curve of a typical tensile test is shown in Fig. 1. The test responses could be compared during each of the sequential test segments. During the initial segment performed at a slow, constant strain rate, specimen often exhibited a rather sharp initial yield point, followed by plastic softening to lower flow stresses. Some tests failed during this test segment at radial strains of less than 1%. For other tests that continued past this strain, the test was switched to a faster constant displacement rate which generated higher stresses and a higher ultimate strength. Initial "slow ultimate strengths" and subsequent "fast ultimate strengths" are compared as functions of temperature for ME3 and Alloy 10 in Fig. 2 and 3. No significant differences in response were observed between DH and PA solution heat treated ME3, based on statistical analyses. Alloy 10 exhibited slightly higher strengths than ME3. The equivalent axial elongation at failure was estimated as 2*radial plastic strain at failure and is compared in Fig. 4. ME3 had significantly higher equivalent axial elongation than Alloy 10 from 1149°C to 1038°C. Both alloys had elongations below 3% from 1038°C down to 815°C, when cooled at 278°C/min. No Alloy 10 specimen cooled at 278°C/min. had sufficient elongation to allow the faster test segment to commence. Alloy 10 specimens cooled at

69°C/min had higher elongations and strengths with decreasing temperature from 1038°C to 815°C. Where comparisons could be made, the strengths measured in these tests were 50-100 MPa lower than those from specimens which were fully heat treated, machined, then conventionally heated up to, stabilized, and tested at the temperature of interest.

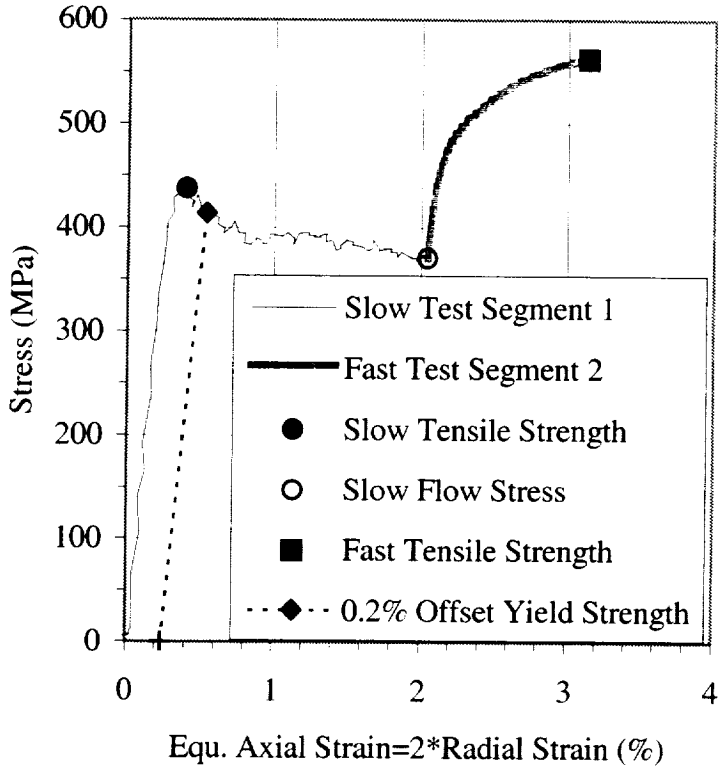

Figure 1. Typical tensile response.

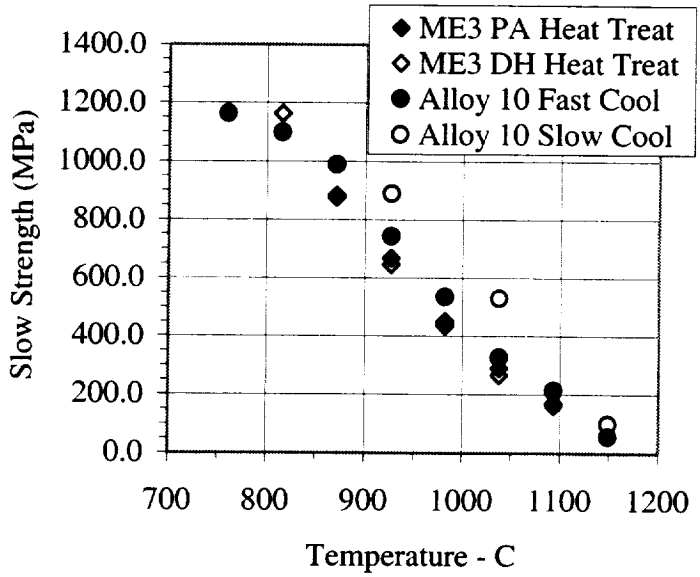

Fig. 2. Comparison of slow tensile strengths.

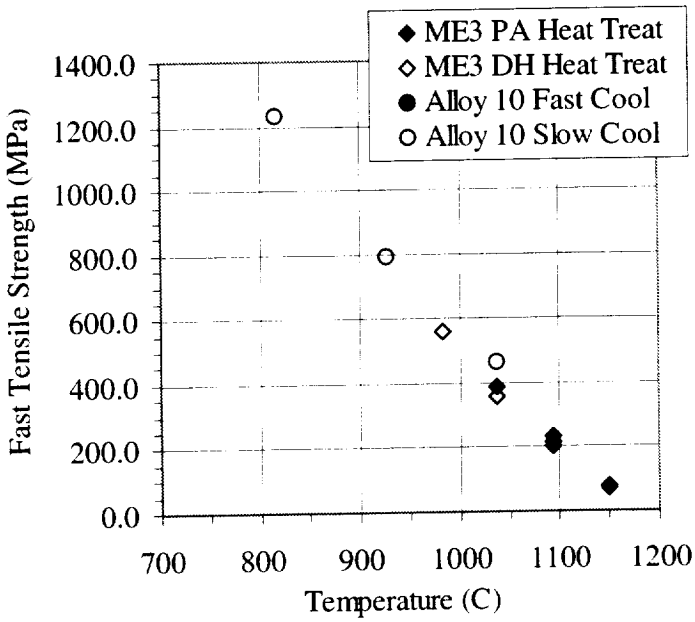

Fig. 3. Comparison of fast tensile strengths; note Alloy 10 Fast Cool specimens failed before reaching the fast test segment 2.

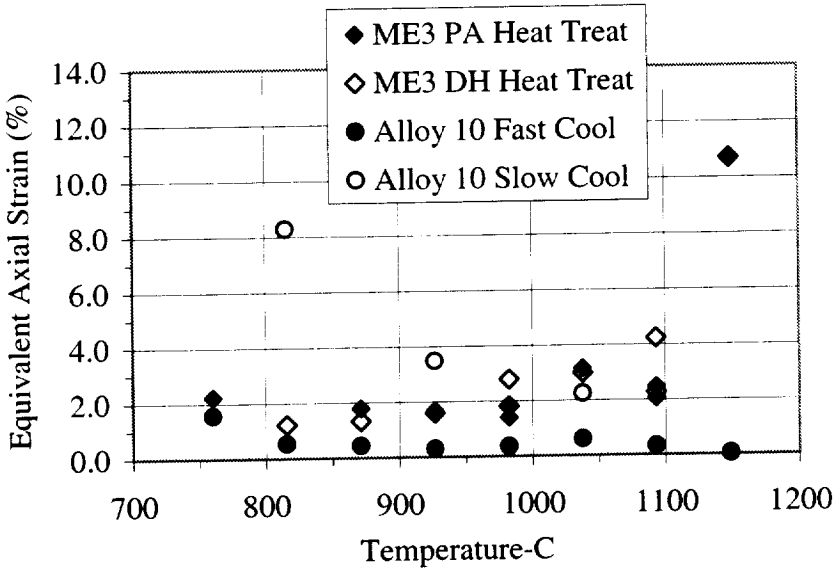

Fig. 4. Comparison of equivalent axial strains at failure.

Failure Mode Evaluations

The failure modes of selected ME3 and Alloy 10 specimens are summarized in Table 1. Typical fracture surfaces for ME3 specimens are compared in Fig. 5. Major cracks usually appeared to be surface-initiated in most specimens, however, evidence of internal secondary cracks with a similar failure mode were sometimes observed. ME3

specimens failed in a mixed transgranular-intergranular mode at 1149°C. At lower temperatures they failed by predominantly intergranular cracking. This response did not vary between PA & DH heat treated specimens.

Alloy 10 specimens failed by predominantly intergranular cracking at all temperatures evaluated at both cooling rates of 69°C/min and 278°C/min, Fig. 6. This intergranular cracking extended through the entire specimen cross-section. For the specimens cooled at the slower rate of 69°C/min., the grain surfaces appeared more textured than those cooled at 278°C/min. This was due to the coarsened gamma prime precipitates observed along the grain boundaries, which could grow during the slower cooling path (ref. 8).

Longitudinal metallographic sections allowed a more complete description of the predominant failure mechanisms. ME3 specimens are shown in Fig. 7. The mixed intergranular-transgranular cracking mode was confirmed on the fracture surfaces of the PA and DH specimens tested at 1149°C. At lower temperatures as typified by the 927°C specimen, a fully intergranular failure path was observed. Observations of secondary cracks indicated cracks formed through joining of cavities nucleating along grain boundaries. The cavities formed along the grain boundaries nearly normal to the loading direction, and were not confined to triple points. These cracks predominantly initiated internally, but sometimes extended to the surface. The necked centers of these specimens had a higher density of these cracks. At 1149°C, the cracks were more widely separated than at lower temperature typified by the 927°C section. This explained the mixed mode failure at 1149°C, where segments of transgranular cracking were necessary to link the separate intergranular cracks to cause failure. The 927°C section displayed more widespread cavitation at grain boundaries and associated secondary cracking there. This allowed failure to occur by the predominant intergranular cracking.

Alloy 10 longitudinal sections are shown in Fig. 8. Unetched and etched pairs of micrographs are shown for each specimen, in order to clearly distinguish between cracks and grain boundaries. Surface and internal cracks were again observed in all Alloy 10 sections examined. However, these cracks appeared to initiate at pores accompanied by a white phase concentrated at triple points and extending along some grain boundaries. The white phase was identified using backscatter scanning electron microscopy as porous eutectic regions of incipient melting. This can be seen clearly in Fig. 8. In the specimens cooled at 278°C/min., these features were observed on random, scattered grain boundaries. However, there were more frequent locations of pores with widespread incipient melting along a majority of the grain boundaries in the center of the specimens cooled at 69°C/min. After etching, this produced a curious macroscopic appearance of concentric rings around the fracture center. Test data indicated temperatures as measured on the specimens' surface were equally well controlled in the 278°C/min. and 69°C/min. tests of Alloy 10. Therefore the widespread incipient melting in specimens cooled at 69°C/min. could be due to a grain boundary instability or a temperature gradient through the cross-section in Alloy 10. These issues are being further explored. No evidence of the widespread incipient melting was observed in the specimen grips, which reflected the microstructural state after the blanks were initially heat treated at the same solution heat treatment temperature as used at the start of the cooling path of the tensile tests.

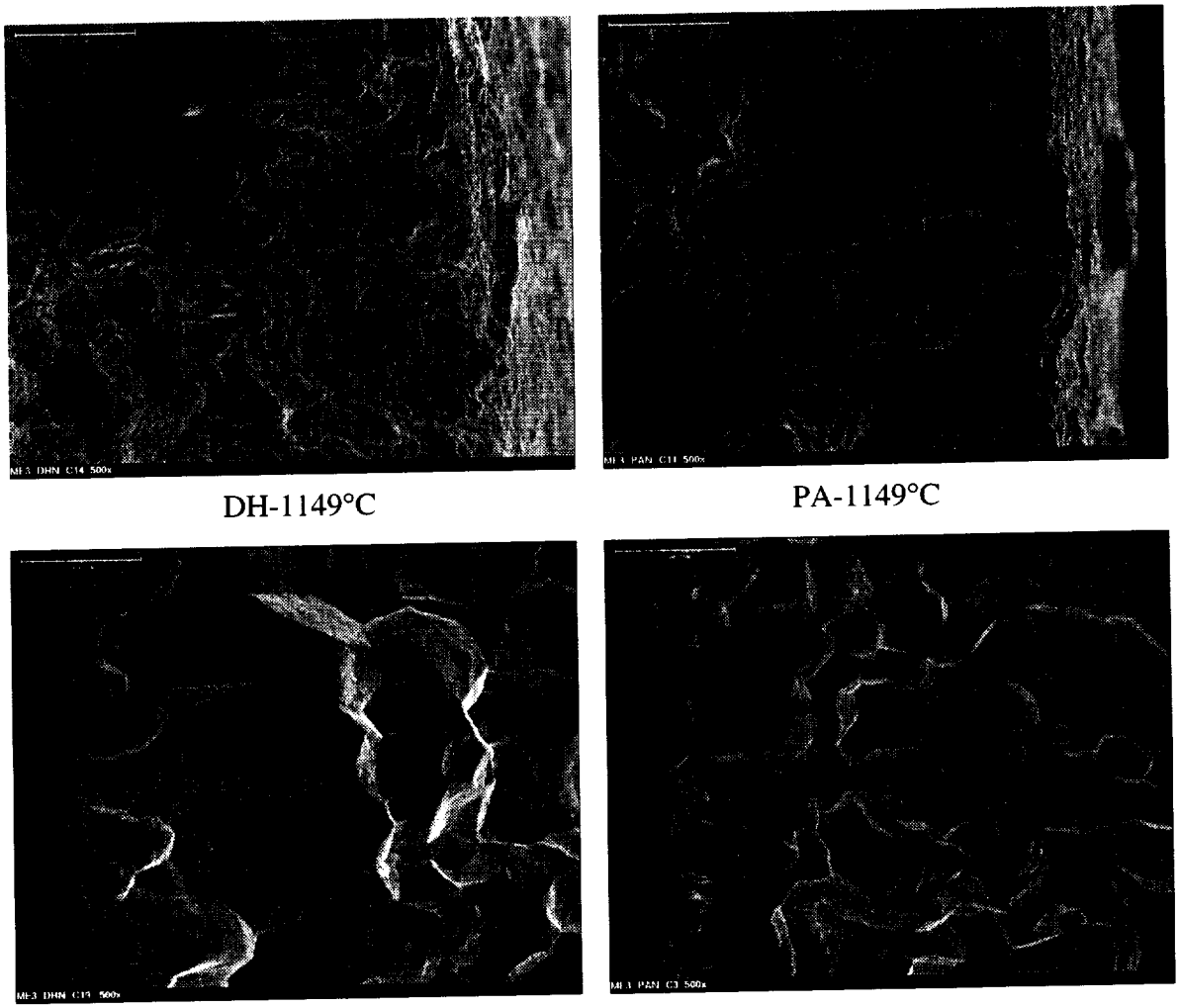

DH-1149°C PA-1149°C

DH-927°C PA-1149°C

Fig. 5. ME3 tensile test failure modes: mixed mode at 1149°C, intergranular at 1149°C.

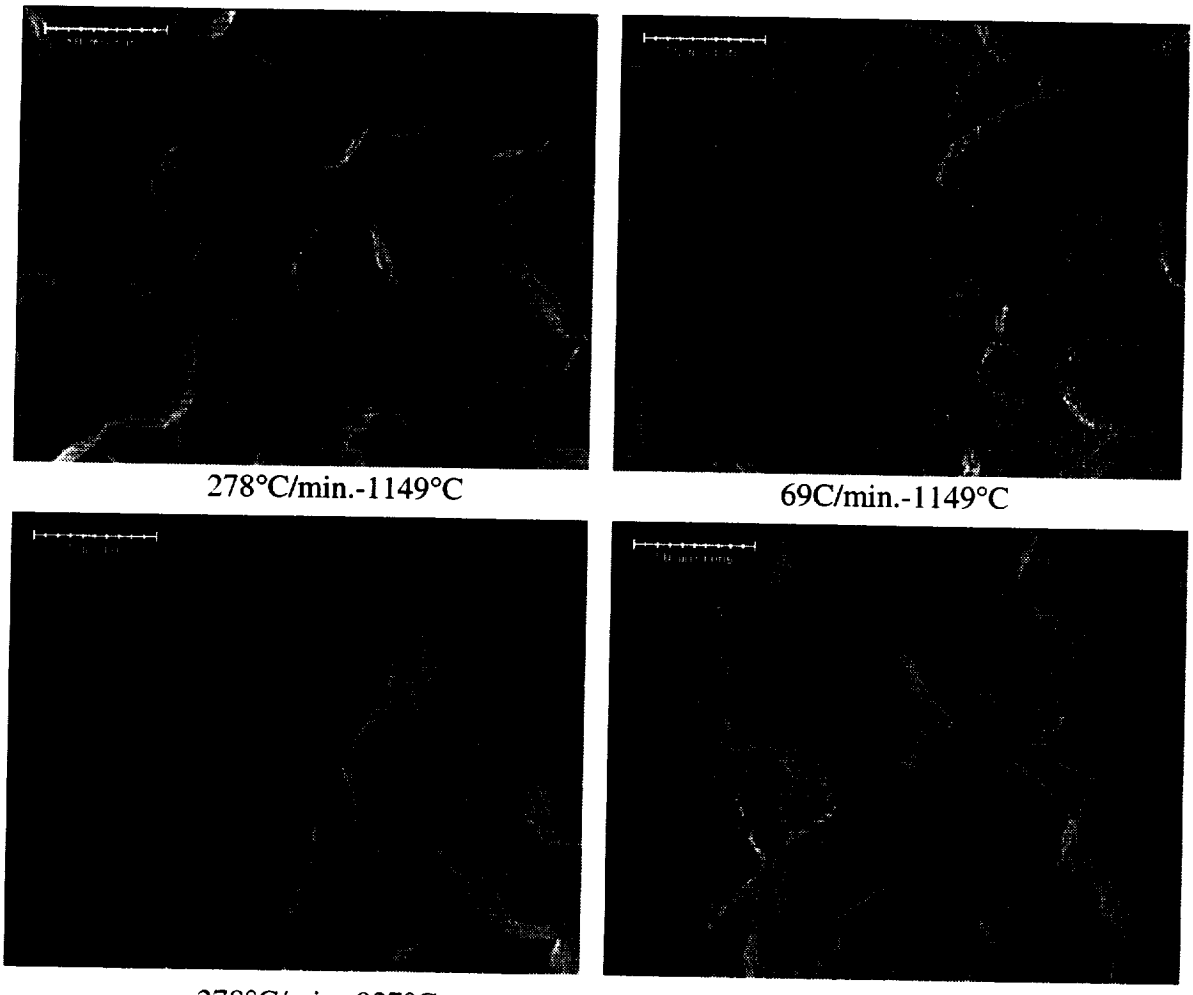

278°C/min.-1149°C

69C/min.-1149°C

278°C/min.-927°C

69°C/min.-927°C

Fig. 6. Alloy 10 tensile test failure modes: intergranular at 1149°C and 927°C.

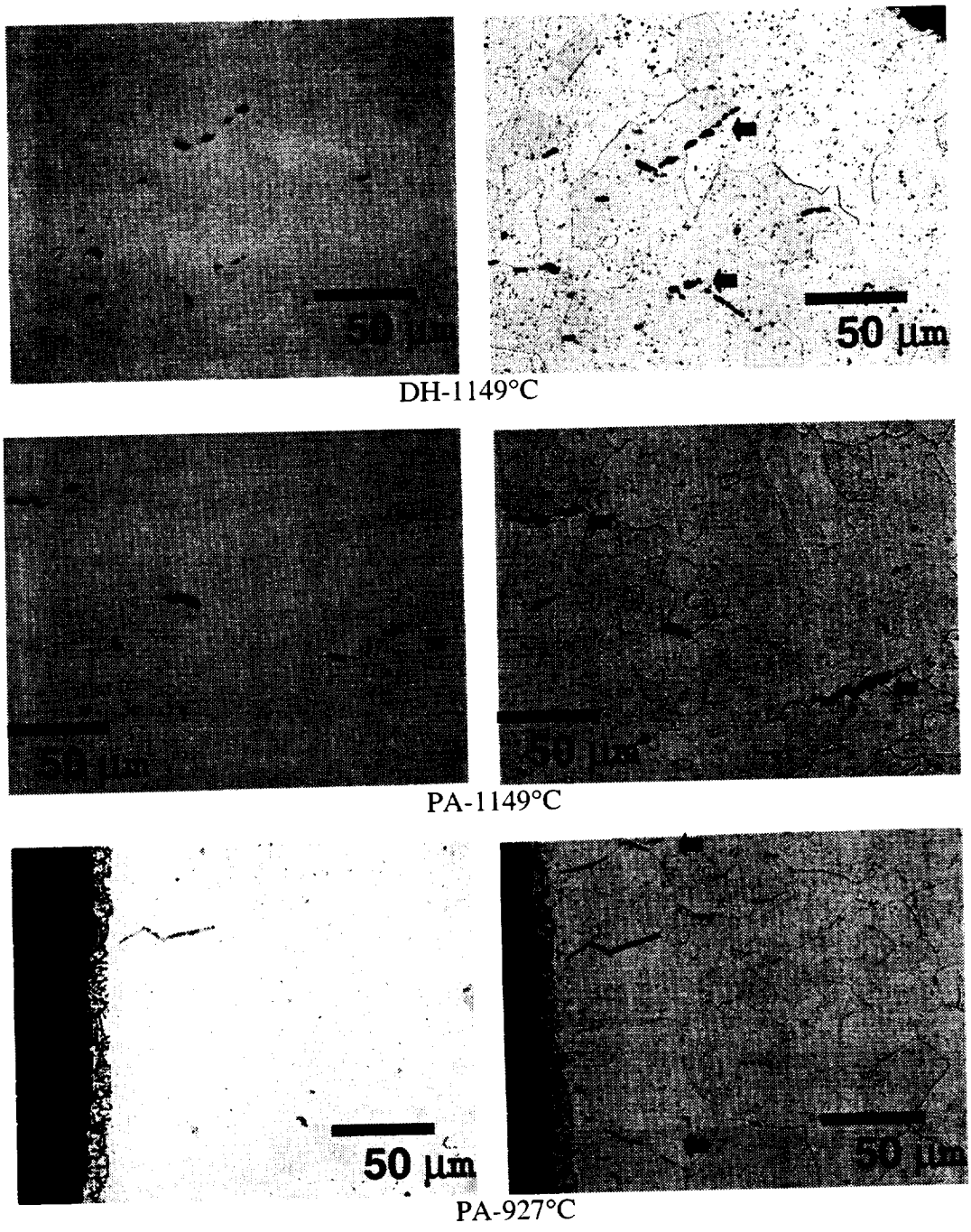

Fig. 7. Secondary cracks at grain boundary cavities (arrows) in ME3 tensile specimen longitudinal sections.

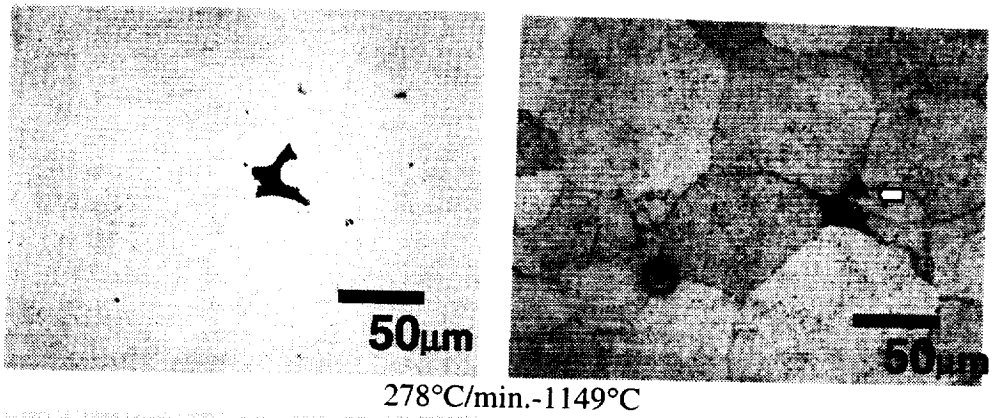

278°C/min.-1149°C

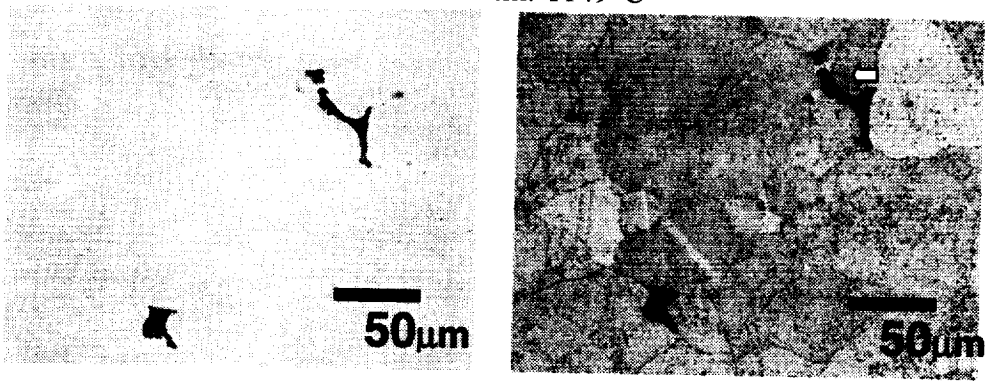

69°C/min.-1149°C

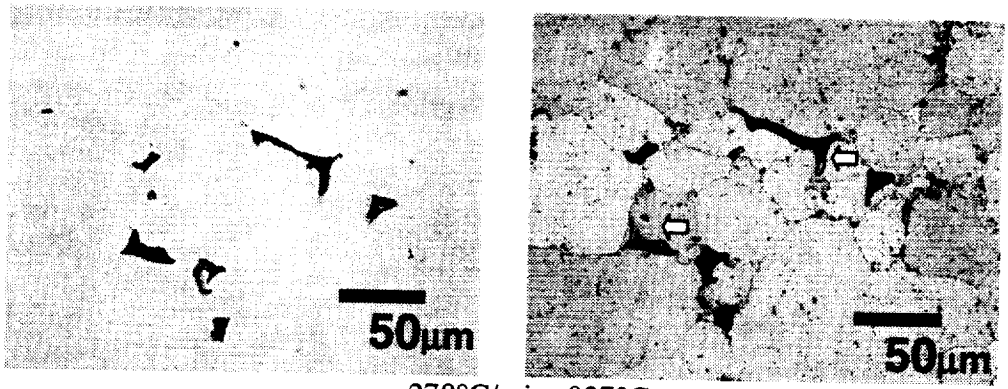

278°C/min.-927°C

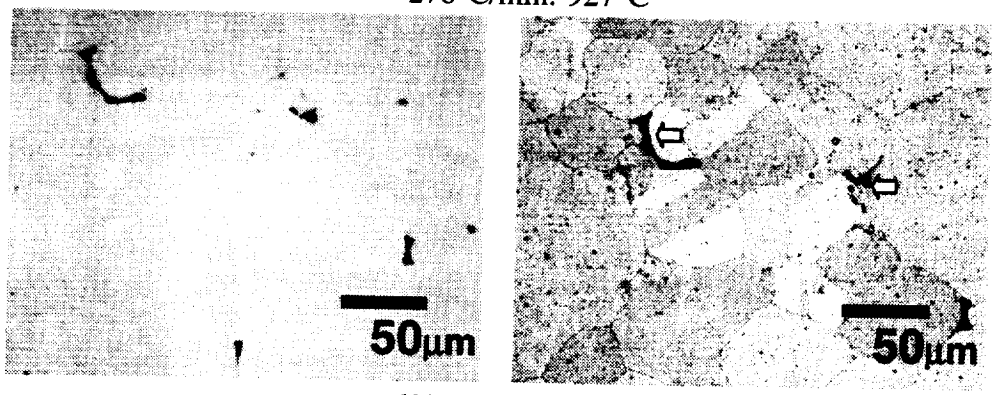

69°C/min.-927°C

Fig. 8. Secondary cracks at incipient melting (arrows) in Alloy 10 longitudinal sections.

Table 1. Comparison of test conditions with elongation and fractography.

Alloy	Solution Heat Treatment	SolutionTemp-°C	Cooling Rate-C/min.	Test Temp-°C	Equiv. Axial Elongation-%	Cracking Mode
ME3	DH	1171	278	1149	10.7	Mixed
ME3	PA	1171	278	1149	10.6	Mixed
ME3	DH	1171	278	1038	3.0	Intergranular
ME3	PA	1171	278	1038	3.2	Intergranular
ME3	DH	1171	278	927	1.6	Intergranular
ME3	PA	1171	278	927	1.7	Intergranular
ME3	DH	1171	278	816	1.2	Intergranular
Alloy 10	PA	1200	278	1149	0.0	Intergranular
Alloy 10	PA	1200	69	1149	0.1	Intergranular
Alloy 10	PA	1200	278	1038	0.6	Intergranular
Alloy 10	PA	1200	69	1038	2.2	Intergranular
Alloy 10	PA	1200	278	927	0.3	Intergranular
Alloy 10	PA	1200	69	927	3.5	Intergranular

Comparison of Quench Cracks in Heat Treated Disks

The fracture surface and longitudinal section of quench cracks found at a very rapidly oil quenched location of an ME3 disk are shown in Fig. 9. The failure was by a mixed intergranular-transgranular mode. The longitudinal section showed other internal cracks forming from cavities along the grain boundaries, very similar to those found in the tensile specimens. This confirmed that grain boundary cavitation was the predominant failure mode in tensile specimens as well as actual rapid quenches of this disk location, in these conditions.

The fracture surface and longitudinal sections of quench cracks found of a fan air quenched Alloy 10 disk are shown in Fig. 10. The failure mode can be seen to be fully intergranular. The fracture surface of the disk interior can be seen to have rounded grain surfaces similar to the Alloy 10 tensile specimens exhibiting widespread incipient melting. A longitudinal section of this crack showed that while the major crack was surface connected, this crack and other secondary cracks appeared to be nucleated internally. A majority of these cracks were associated with sites on the grain boundary containing evidence of incipient melting. This indicated that cracking at incipient melting sites was the operative failure mode during tensile tests as well as actual quenches of Alloy 10 disks in these conditions.

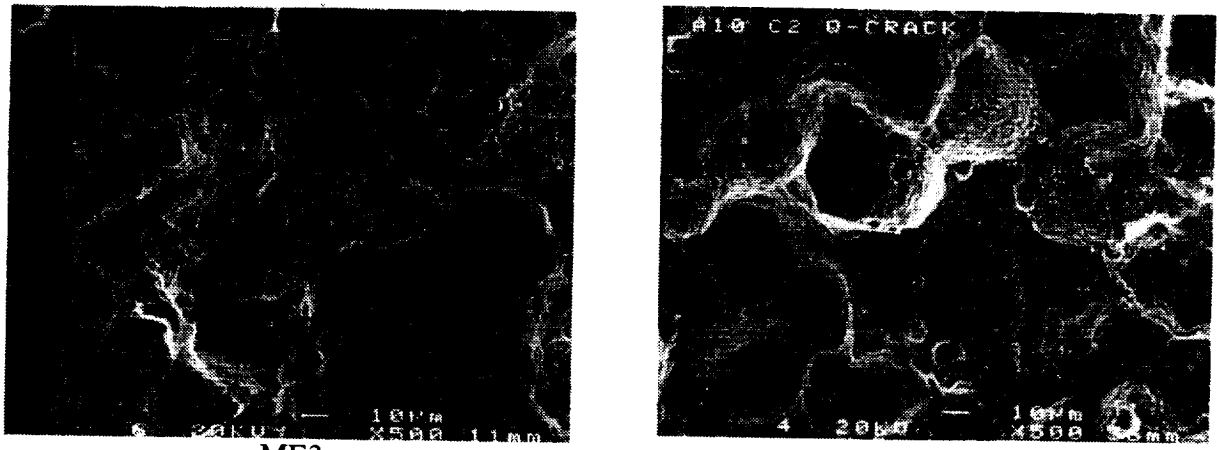

ME3 Alloy 10

Fig. 9. ME3 and Alloy 10 quench crack surfaces.

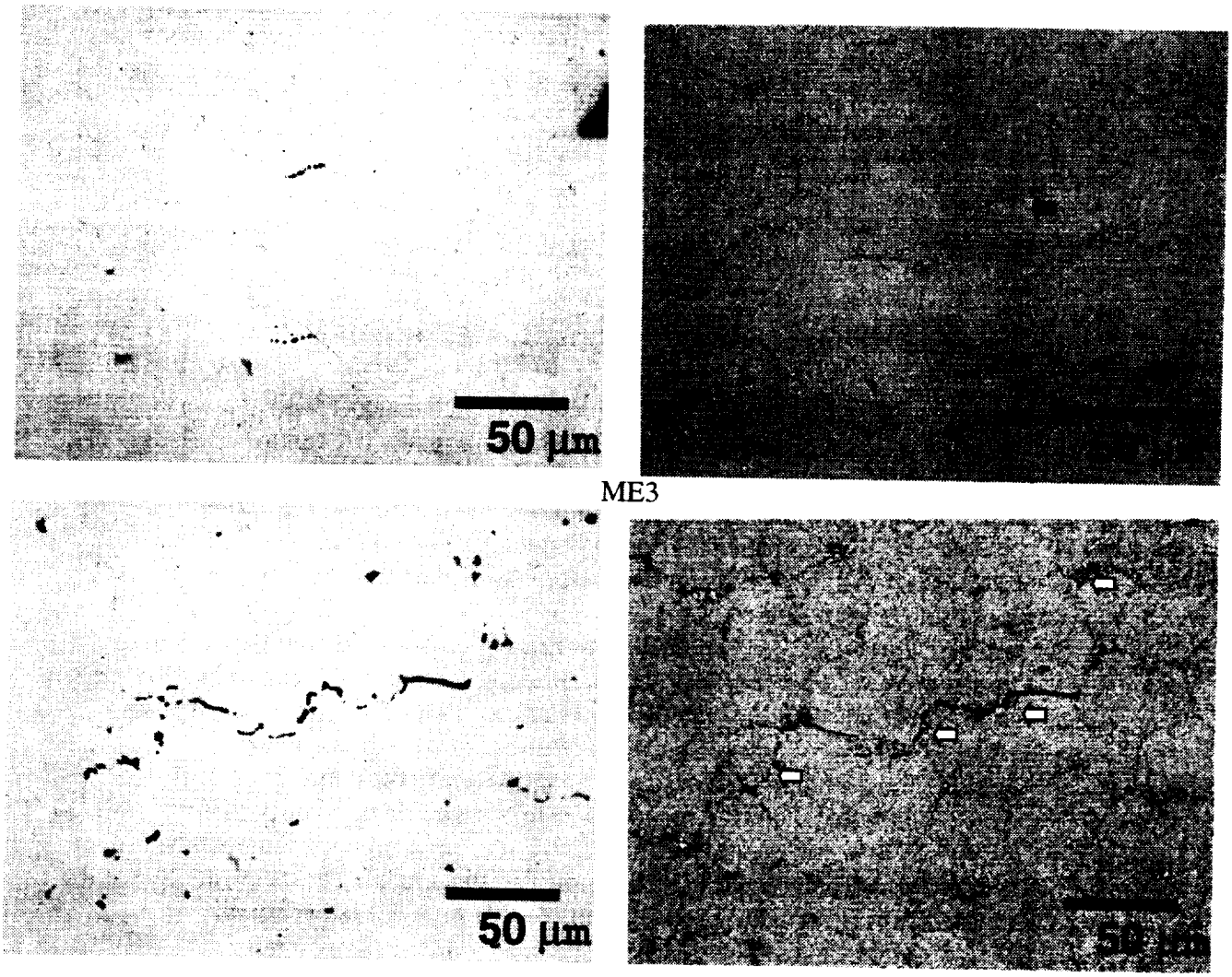

ME3

Alloy 10

Fig. 10. ME3 and Alloy 10 disk secondary quench cracks in longitudinal sections.

SUMMARY AND CONCLUSIONS

A series of tensile tests were performed in simulated quenching conditions for disk alloys ME3 and Alloy 10 after supersolvus heat treatments. The findings can be summarized as follows:

1) Alloy 10 had slightly higher strengths than ME3 in tensile tests performed during simulated quench heat treatments. This superior strength increased with decreasing cooling rate.
2) ME3 had significantly higher ductility than Alloy 10 at temperatures approaching the solution heat treatment. This superior ductility did not vary between alternative solution heat treatments DH and PA.
3) The differences in ductility were associated with different failure modes: cavitation at grain boundaries in ME3 and cracking from porosity and incipient melting at grain boundaries in Alloy 10.
4) Evidence of these failure modes was observed in quench cracks of disks for both alloys.

It can be concluded from this work that:

1) Supersolvus heat treated ME3 is more resistant to quench cracking because of its higher ductility near its solution temperature. The associated failure mode is cavity nucleation at the grain boundaries normal to the stress axis. However, at temperatures near 1149°C, these cavities are widely scattered enough to allow some transgranular crack linkage, and significantly ductility. This failure mode is not sensitive to heat treatment solution time variations of 1-3 h possible in large disks, but could vary with quenching rate.
2) Supersolvus heat treated Alloy 10 is less resistant to quench cracking because of its low ductility near its solution temperature. The associated failure mode is fully intergranular cracking from pores and incipient melting locations along the grain boundaries. This low ductility failure mode appeared accentuated with slower cooling rates, however this effect is the subject of further evaluations.
3) On-cooling tensile tests can faithfully capture many essential features responsible for quench cracking of disks: measured strengths, ductilities, failure modes and alloy rankings consistent with results from actual disks.

REFERENCES

1. T. P. Gabb, J. Gayda, J. Telesman, "Development of Advanced Powder Metallurgy Disk Alloys in NASA-Industry Programs", Aeromat 2001, Long Beach, CA, June 14, 2001.
2. J. Gayda, "Alloy 10: A 1300°F Disk Alloy", NASA TM-210810, Washington, D.C., 2001.
3. S. K. Jain, "High OPR Core Material (AoI 4.2.4), Regional Engine Disk Development"AST Regional Disk Program Final Report, NAS3-27720, Nov. 1999.

4. R. F. Decker, "Strengthening Mechanisms in Nickel-Base Superalloys", Proc. of Steel Strengthening Mechanisms Symposium, May 5-6, 1969, Zurich, Switzerland, Climax Molybdenum Co., 1969.
5. D. R. Chang, D. D. Krueger, R. A. Sprague, "Superalloy Powder Processing, Properties and Turbine Disk Applications", in Superalloys 1984, ed. M. Gell, C. S. Kortovich, R. H. Bricknell, W. B. Kent, J. F. Radavich, TMS-AIME , Warrendale, PA, 1984, pp. 245-273.
6. J. R. Groh, "Effect of Cooling Rate From Solution Heat Treatment on Waspaloy Microstructure and Properties", in Superalloys 1996, ed. R. D. Kissinger, D. J. Deye, D. L. Anton, A. D. Cetel, M. V. Nathal, T. M. Pollock, D. A. Woodford, TMS-AIME, Warrendale, PA, 1996, pp. 621-626.
7. R. D. Kissinger, "Cooling Path Dependent Behavior of a Supersolvus Heat Treated Nickel Base Superalloy", in Superalloys 1996, ed. R. D. Kissinger, D. J. Deye, D. L. Anton, A. D. Cetel, M. V. Nathal, T. M. Pollock, D. A. Woodford, TMS-AIME, Warrendale, PA, 1996, pp.687-696.
8. A. K. Koul, G. H. Gessinger, "On the Mechanism of Serrated Grain Boundary Formation in Ni-Based Superalloys", Acta Metallurgica, V. 31, 1983, pp. 1061-1069.

REPORT DOCUMENTATION PAGE

Form Approved
OMB No. 0704-0188

1. AGENCY USE ONLY (Leave blank)	2. REPORT DATE	3. REPORT TYPE AND DATES COVERED
	October 2001	Technical Memorandum

4. TITLE AND SUBTITLE

The Tensile Properties of Advanced Nickel-Base Disk Superalloys During Quenching Heat Treatments

5. FUNDING NUMBERS

WU-714-04-10-00

6. AUTHOR(S)

Timothy P. Gabb, John Gayda, Pete T. Kantzos, Tiffany Biles, and William Konkel

7. PERFORMING ORGANIZATION NAME(S) AND ADDRESS(ES)

National Aeronautics and Space Administration
John H. Glenn Research Center at Lewis Field
Cleveland, Ohio 44135-3191

8. PERFORMING ORGANIZATION REPORT NUMBER

E-13070

9. SPONSORING/MONITORING AGENCY NAME(S) AND ADDRESS(ES)

National Aeronautics and Space Administration
Washington, DC 20546-0001

10. SPONSORING/MONITORING AGENCY REPORT NUMBER

NASA TM—2001-211218

11. SUPPLEMENTARY NOTES

Prepared for the 2001 Fall Meeting sponsored by The Minerals, Metals, and Materials Society, Indianapolis, Indiana, November 4–8, 2001. Timothy P. Gabb and John Gayda, NASA Glenn Research Center; Pete T. Kantzos, Ohio Aerospace Institute, 22800 Cedar Point Road, Brook Park, Ohio 44142; Tiffany Biles, Purdue University, West Lafayette, Indiana 47907–1968; and William Konkel, Wyman-Gordon Forgings, Houston, Texas 77095. Responsible person, Timothy P. Gabb, organization code 5120, 216–433–3272.

12a. DISTRIBUTION/AVAILABILITY STATEMENT

Unclassified - Unlimited
Subject Category: 26 Distribution: Nonstandard

Available electronically at http://gltrs.grc.nasa.gov/GLTRS

This publication is available from the NASA Center for AeroSpace Information, 301–621–0390.

12b. DISTRIBUTION CODE

13. ABSTRACT ***(Maximum 200 words)***

There is a need to increase the temperature capabilities of superalloy turbine disks. This would allow full utilization of higher temperature combustor and airfoil concepts under development. One approach to meet this goal is to modify the processing and chemistry of advanced alloys, while preserving the ability to use rapid cooling supersolvus heat treatments to achieve coarse grain, fine gamma prime microstructures. An important step in this effort is to understand the key high temperature tensile properties of advanced alloys as they exist during supersolvus heat treatments. This could help in projecting cracking tendencies of disks during quenches from supersolvus heat treatments. The objective of this study was to examine the tensile properties of two advanced disk superalloys during simulated quenching heat treatments. Specimens were cooled from the solution heat treatment temperatures at controlled rates, interrupted, and immediately tensile tested at various temperatures. The responses and failure modes were compared and related to the quench cracking tendencies of disk forgings.

14. SUBJECT TERMS

Superalloy; Disk; Quenching

15. NUMBER OF PAGES

20

16. PRICE CODE

17. SECURITY CLASSIFICATION OF REPORT	18. SECURITY CLASSIFICATION OF THIS PAGE	19. SECURITY CLASSIFICATION OF ABSTRACT	20. LIMITATION OF ABSTRACT
Unclassified	Unclassified	Unclassified	